

- <sup>3</sup>A. Jayaraman, R. G. Maines, and L. D. Longinotto, *Bull. Am. Phys. Soc.* **22**, 292 (1977).
- <sup>4</sup>L. D. Finkel'shtein, N. N. Efremova, N. I. Lobachevsaya, S. A. Nemnonov, and V. G. Bamburov, *Fiz. Tverd. Tela (Leningrad)* **18**, 3117 (1976) [*Sov. Phys. Solid State* **18**, 1818 (1976)].
- <sup>5</sup>A. E. Sovestnov, G. A. Krutov, A. S. Ryl'nikov, and V. A. Shaburov, *Zh. Eksp. Teor. Fiz.* **73**, 961 (1977) [*Sov. Phys. JETP* **46**, 507 (1977)].

- <sup>6</sup>*Fizicheskie svoystva khal'kogenidov redkozemel'nykh elementov (Physical Properties of the Chalcogenides of Rare-Earth Elements)*, Nauka, Leningrad, 1973.
- <sup>7</sup>R. S. Erofeev, N. V. Kolomets, and V. N. Ovechkin, *Izv. Akad. Nauk SSSR, Neorg. Mater.* **13**, 978 (1977).
- <sup>8</sup>B. I. Shklovskii and A. L. Éfros, *Usp. Fiz. Nauk* **117**, 401 (1975) [*Sov. Phys. Usp.* **18**, 845 (1975)].

Translated by J. G. Adashko

## Elastic and inelastic scattering of Mössbauer $\gamma$ quanta in a pyrolytic graphite crystal

N. N. Lobanov, V. A. Bushuev, V. S. Zasimov, and R. N. Kuz'min

*Moscow State University*

(Submitted 20 September 1978)

*Zh. Eksp. Teor. Fiz.* **76**, 1128–1135 (March 1979)

A method free of systematic errors is proposed for the measurement of the intensity of elastic and inelastic scattering of Mössbauer  $\gamma$  quanta in substances that do not contain resonant nuclei and can be in arbitrary aggregate states. The method was used to measure the intensity of elastic and inelastic scattering of 14.4 keV Mössbauer radiation along the profile of the (002) Bragg reflection and at the maxima of the reflections (004), (006), and (008) in a crystal of highly oriented pyrolytic graphite. It is shown that the existing theory of elastic scattering of x rays in mosaic crystals, as well as the theory of thermal diffuse and Compton scattering, can describe satisfactorily the experimental results. The shear modulus  $c_{44}$  and the law governing the mosaic distribution are determined, and the dimensions of the coherently scattering blocks are estimated.

PACS numbers: 76.80. + y.

### INTRODUCTION

Among the widely known methods of investigating the structure of matter and elementary excitations, such as elastic and inelastic scattering of x rays and thermal neutrons, a special place is occupied by the study of the scattering of Mössbauer  $\gamma$  radiation in a substance that contains no resonant nuclei, owing to the high resolution of this method ( $\sim 10^{-8}$  eV). The main idea underlying such experiments is that the Mössbauer radiation scattered from the sample is analyzed by a resonant absorber placed ahead of the detector.<sup>1-3</sup>

Despite the simplicity and elegance of the described<sup>1-3</sup> methods, a number of questions remain unanswered. These involve the allowance for the systematic errors when the background is determined and the calculation of the instrumental errors. The latter occur mainly because the luminosity of the instrument must be increased, and this leads to deviation from Bragg focusing in the Mössbauer diffractometer. This question was analyzed in detail in Ref. 4, where modifications of the procedures of Refs. 1–3 were proposed, aimed at eliminating the systematic errors in the determination of the background.

In the present study we have measured by the procedure of Ref. 4 the intensities of the elastic and inelastic scattering of 14.4-keV Mössbauer  $\gamma$  quanta in a highly oriented pyrolytic graphite (PG) crystal. The

main structural units of this graphite are planar atomic grids in which the hydrogen atoms are located at the corners of regular hexagons. These grids are arranged in an ABABAB... sequence as in natural graphite, forming stacks turned randomly relative to one another in the planes of the grids. Despite the considerable progress in the production of PG, it has been impossible to grow sizable artificial single crystals. It is therefore very important to accumulate experimental data on such important physical characteristics of graphite as the thickness of the stacks with regular packing and the elastic constants, particularly  $c_{44}$  (the shear modulus, which determines the critical fracture stress perpendicular to the  $c$  axis). In fact, the dimensions of the stacks with regular packing and their degree of disorientation determine the angle widths of the elastic-scattering reflections, while the elastic constants can be determined by measuring the intensity of the thermal diffuse scattering (TDS) in Bragg reflections.

Nondestructive control methods such as x-ray and  $\gamma$ -ray scattering are particularly attractive. Traditional measurements of the elastic constants by ultrasonic and static methods require samples of appreciable size and of special shape, whereas the method proposed by us is free of these limitations. As to the purely scientific problems, the study of graphite is of interest from the point of view of checking on the present theories of secondary extinction in TDS, inasmuch as the ex-

tion attenuation in graphite exceeds the photoelectric absorption, and this must also be taken into account in the calculation of the inelastic-scattering intensity near the Bragg maxima; graphite is characterized by an appreciable anisotropy of the force constants. The region of applicability of our method is not confined to the solution of the problems indicated above, and it can be used to measure elastic and inelastic scattering intensities in other substances in arbitrary aggregate states.

## 1. EXPERIMENTAL PROCEDURE

The experimental setup for the measurements of the elastic and inelastic scattering intensity is based on the GUR-4 goniometer. The primary gamma beam had horizontal and vertical divergences  $0.78^\circ$  and  $0.95^\circ$  respectively. The detector solid angle was  $\Delta\Omega = 8.62 \times 10^{-3}$  sr. A  $^{57}\text{Co}$  (Pd) source was used in the experiment. The resonant absorber was iron foil  $6 \mu\text{m}$  thick, enriched to 80% of  $^{57}\text{Fe}$ .

The measurement procedure was the following. We first determined the intensity of the primary beam, using the setup a shown in the figure. To this end we measured the intensities  $I_r(0)$  and  $I_n(0)$  of the radiation in the case when the source velocity  $v$  relative to the absorber was equal to the resonant value ( $v=r$ ) and to the nonresonant one ( $v=n$ ), respectively. In this experiment the intensity of the primary beam was taken to be the difference

$$I_{00} = I_n(0) - I_r(0) = (\varphi_n - \varphi_r) \eta f_s I_0, \quad (1)$$

where  $I_0$  is the intensity of the  $\gamma$  radiation of the Mössbauer transition with energy  $E_0$ ;  $f_s$  is the probability of the Mössbauer effect in the source;  $\eta = \exp(-\mu x)$ , and similarly  $\eta_E = \exp(-\mu_E x)$ , where  $\mu$  and  $\mu_E$  are the linear coefficients of the photoelectric absorption of the Mössbauer  $\gamma$  radiation and of the background emission  $I_E$  coming from a source of energy  $E$  and falling in the detector pass band;  $x$  is the thickness of the resonant absorber, and  $\varphi_v = \exp(-\mu_v x)$ , where  $\mu_v$  is the linear coefficient of the resonant absorption.

The experiment was next performed in accordance with setups b and c in the figure. If the source velocity relative to the absorber is  $v$ , then in the case b the detector registers an intensity

$$I_{1v}(2\theta) = (1 - pf_s) \eta b_0 I_0 + \varphi_v \eta b_0 p f_s I_0 + \eta_E b_E I_E + I'_1 + I', \quad (2)$$

and in case c

$$I_{2v}(2\theta) = (1 - f_s) \eta b_0 I_0 + \varphi_v \eta b_0 f_s I_0 + \eta_E b_E I_E + I'_2 + I', \quad (3)$$

here  $b_0$  and  $b_E$  are the reflection coefficients of  $\gamma$  quanta of energy  $E_0$  and  $E$  respectively at a scattering angle  $2\theta$ ,  $p$  is the ratio of the elastic-scattering intensity of the Mössbauer radiation to the total scattering intensity of this radiation at the angle  $2\theta$ ,  $I'$  is the intensity of the false signals in the electric circuits of the setup and of the cosmic background, and  $I'_1$  and  $I'_2$  are the counting rates resulting from the  $\gamma$  radiation of the impurities in the resonant absorber.

Measurements of the counting rates at resonance and off-resonance in cases b and c yield

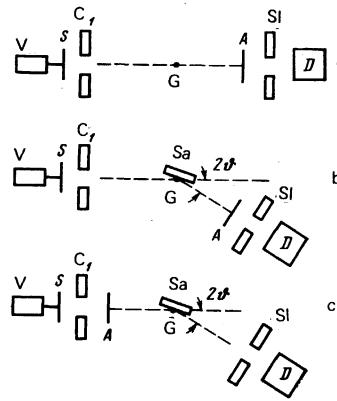


FIG. 1. Experimental setups for the investigation of elastic and inelastic scattering of  $\gamma$  quanta in crystals by the Mössbauer effect. V—electrodynamic vibrator, S—source of  $\gamma$  quanta, D—detector,  $C_1$ —collimator, S1—receiving slit of detector, Sa—investigated sample, A—resonant absorber, G—vertical axis of goniometer.

$$\begin{aligned} I_1 &= I_{1n}(2\theta) - I_{1r}(2\theta) = b_0 p (\varphi_n - \varphi_r) \eta f_s I_0, \\ I_2 &= I_{2n}(2\theta) - I_{2r}(2\theta) = b_0 (\varphi_n - \varphi_r) \eta f_s I_0. \end{aligned} \quad (4)$$

The sought quantities  $b_0 p$  and  $b_0(1-p)$  are thus respectively equal to  $I_1/I_{00}$  and  $(I_2 - I_1)/I_{00}$ .

The proposed procedure is superior to that of Refs. 1–3 since there is no need here to measure the background intensity in the primary and reflected beams  $I_E$  and  $b_E I_E$ , or the intensities  $I'$ ,  $I'_1$  and  $I'_2$ , nor is it necessary to estimate  $\eta$ ,  $\eta_E$ ,  $\varphi_n$ ,  $\varphi_r$ ,  $f_s$ , and  $I_0$ , all of which must be done according to Refs. 1–3; it is necessary, just as there, to take into account the finite half-life of the source. The greatest difficulties in the procedures of Refs. 1–3 arise in the measurements of  $I_E$  and  $b_E I_E$ , and especially in the estimate of their errors, since the source background radiation is not monoenergetic, and this leads to systematic errors that have not been estimated. Additional errors arise also in the measurements of the remaining parameters.

## 2. EXPERIMENTAL RESULTS AND DISCUSSION

a) *Elastic scattering.* We used a highly oriented PG sample measuring  $20 \times 20 \times 3.5$  mm. The x-ray diffraction analysis was performed with an URS-50 diffractometer in  $\text{CuK}\alpha$  radiation, with monochromatic reflection from the  $10\bar{1}1$  planes of ideal quartz. Registration was with an SSS single-channel analyzer and an SRS-1.0 detector.

The investigations have shown that the sample contains an axial structure whose axis is parallel to the  $c$  axis and whose unit cell is hexagonal with parameters  $a = 2.461 \pm 0.002 \text{ \AA}$ ,  $c = 6.708 \pm 0.006 \text{ \AA}$ . The errors cited here and hereafter are the variances of the measurement results. The same installation was used to obtain by the  $\omega$  method the rocking curve of the (002) reflection. The scanning region was  $\pm 1.5^\circ$ , the width of the curve at half maximum was  $\varepsilon_{0.5} = 54' \pm 2'$ , and the integrated reflection coefficient was  $R_{\text{Cu}} = (4.70 \pm 0.08) \cdot 10^{-3}$ . Prior to the measurements of the elastic and inelastic scattering intensities we determined the linear coef-

efficient  $\mu = 1.783 \pm 0.002 \text{ cm}^{-1}$  of the photoelectric absorption of 14.4-keV  $\gamma$  quanta in the investigated sample from the absorption of resonant  $\gamma$  radiation monochromatized beforehand by reflection from the (002) planes of the PG.

The integrated coefficient of elastic (002) scattering of the  $\gamma$  quanta was determined by the procedure (1)–(4) described above using the standard  $\omega$ -scanning scheme. The scanning region was  $\pm 2^\circ$ , the scanning step was  $10'$ , and the width of the curve at half maximum was  $1.7^\circ$ . The measured value was  $R_{Co} = (6.99 \pm 0.07) \cdot 10^{-3}$ . The elastic scattering was measured also at the maxima of the Bragg reflections (004), (006), and (008). The experimental results normalized to the intensity  $I_{00}$  are listed in Table I. In the calculation we took into account, in accord with Ref. 4, the instrumental errors resulting from non-Bragg focusing.

In the symmetrical Bragg case, the reflection coefficient  $K(\epsilon)$  ( $\epsilon$  is the deviation from the exact Bragg angle  $\vartheta_0$ ) was calculated using the approach developed in Ref. 5. The distribution of the normals to the reflecting planes of the mosaic blocks was assumed Gaussian. Next, following Ref. 4, the instrumental errors were taken into account.

In practice it is frequently customary to use two approximations: 1) the case when secondary extinction can be neglected (kinematic approximation), i.e.,  $\sigma/\mu \ll 1$ , where  $\sigma(\epsilon)$  is the reflectivity of the crystal per unit length<sup>5</sup>; 2) the thick-crystal approximation, when  $\mu l_1/\sin\vartheta_0 \gg 1$ , where  $l_1$  is the sample thickness. The corresponding reflection coefficients will be designated  $K_1(\epsilon)$  and  $K_2(\epsilon)$ . The exact solution with account taken of the secondary extinction and of the finite crystal thickness will be designated for convenience  $K_3(\epsilon)$ . The integrated reflection coefficients in the very same approximation is equal to  $R_i = \int K_i(\epsilon) d\epsilon$ , where the integration limits are determined by the scanning region. The values of  $K_i$  and  $R_i$  will hereafter be compared with the experimental results.

For a more correct interpretation of the results obtained with  $\gamma$  rays, we have analyzed beforehand the data on the intensity of elastic scattering of  $\text{CuK}\alpha$  radiation, since the intensity of inelastic scattering of the (002) Bragg reflection has been shown by experiments with  $^{57}\text{Co}$   $\gamma$  radiation to be less than the measurement errors (see Table II). An analysis of the exact expression for  $K_3(\epsilon)$  shows that secondary extinction makes the width of the rocking curve larger than the width of the true distribution of the mosaic blocks. In fact, a

TABLE I. Elastic-scattering coefficients at the maxima of the Bragg reflections {00l} of PG using Mössbauer  $\gamma$  radiation of  $\text{Co}^{57}(\text{Pd})$ .  $K_e$  and  $\sigma_e$  are the experimental results and the variance.

hkl	$K_1 \cdot 10^3$	$K_2 \cdot 10^3$	$K_3 \cdot 10^3$	$K_e \cdot 10^3$	$\sigma_e \cdot 10^4$
0 0 2	60.6	29.8	29.8	22.8	14
0 0 4	8.93	8.01	7.58	4.96	4.3
0 0 6	2.55	2.60	2.14	1.03	1.2
0 0 8	1.07	1.12	0.80	0.26	0.6

TABLE II. Inelastic-scattering coefficients at the maxima of the Bragg reflections {00l} of PG using Mössbauer  $\gamma$  radiation of  $\text{Co}^{57}(\text{Pd})$ .  $N$  and  $\sigma_e$  are the experimental results and variance.

hkl	$R_C \cdot 10^3$	$R_T^{(1)} \cdot 10^3$	$k$	$R_{inel} \cdot 10^3$	$N \cdot 10^3$	$\sigma_e \cdot 10^3$
0 0 2	4.87	1.63	1.02	1.71	0.0	2.0
0 0 4	12.12	1.49	1.05	1.69	2.6	0.6
0 0 6	6.66	1.13	1.10	1.31	1.3	0.2
0 0 8	5.01	0.92	1.14	1.10	0.96	0.09

numerical solution of the equations  $K_i(\epsilon, \delta/2) = 0.5K_i(0)$  yielded the mosaic-distribution parameters  $g_1 = 43$ ,  $g_2 = g_3 = 51.2$ . The constants used in the calculations were taken from the tables of Ref. 6.

The calculations show that it is impossible to obtain in the kinematic approximation agreement with the results of measurements with  $\text{CuK}\alpha$  radiation ( $R_i = 7.78 \cdot 10^{-3}$ ), whereas the profiles and integrated reflection coefficients in case 2 and in the case of the exact solution agree with experiment ( $R_2 = R_3 = 4.71 \cdot 10^{-3}$ ). The fact that the last two approximations yield the same result is not unexpected, since  $\mu = 9.246 \text{ cm}^{-1}$  (Ref. 7) and  $\mu l_1/\sin\vartheta_0 = 14.08$ . We note that the relation frequently used in practice for  $K_1$  of PG is incorrect, since the ratio at the maximum of the (002) Bragg reflection is  $\sigma(0)/\mu = 1.275$  for  $\text{CuK}\alpha$  radiation.

The preceding results were obtained under the assumption that the PG crystal is of the first type in the Zachariasen classification,<sup>5</sup> i.e.,  $\delta = g\lambda/l_0 \cos\vartheta_0 \ll 1$ , where  $\lambda$  is the wavelength and  $l_0$  is the average thickness of the mosaic blocks. Starting from the experimental errors in the determination of the  $K_3$  profile, this inequality can be made more accurate:  $\delta \leq 10^{-2}$ . Therefore, taking into account the experimentally determined  $g = 51.2$ , we find that the dimensions of the coherently scattering blocks along the  $c$  axis and in the perpendicular direction can be estimated respectively at  $l_{0c} = l_0 \sin\vartheta_0 \geq 570 \text{ \AA}$  and  $l_{0a} = l_0 \cos\vartheta_0 \geq 4400 \text{ \AA}$ . The lower limit of the  $c$  dimension of the crystallites was determined by the density of the stacking faults in the graphite, which lead at an appreciable density to turbostratified disorder; the fraction of the turbostratified planes at  $l_{0c} \geq 570 \text{ \AA}$  is therefore  $p_i \leq 5.9 \cdot 10^{-3}$ , in good agreement with the value  $p_1$  calculated with Bacon's empirical formula<sup>8</sup> for our measured value of  $c$ .

It follows from our experimental results on Mössbauer radiation that the profiles of the (002) reflection, calculated for  $K_2$  and  $K_3$ , agree with experiment. Nonetheless, for the maxima of the remaining Bragg reflections the  $K_3$  profile is in better agreement with experiment than  $K_2$ , owing to the decrease of the effective sample thickness with increasing order of the reflection (see Table I). With increasing scattering angle, the disparity between theory and experiment increases, a fact explained by the increase of the contribution of the second-order terms which were not taken into account in the estimate of the instrumental errors. The calculated coefficients of the integrated (002) reflection agree satisfactorily with experiment both in the stepwise and in the continuous scanning approximation

$$(R_3 = 6.53 \cdot 10^{-3}).$$

Measurement of the intensities of elastic scattering of the  $\gamma$  radiation of  $^{57}\text{Co}$  shows thus a satisfactory agreement between theory and experiment, and this allows us to draw the following conclusions: 1) The existing theory of secondary extinction describes adequately the experimental results on elastic scattering of x rays and gamma rays in PG. 2) The crystallites in the investigated PG sample are quite sizable ( $l_{0c} \geq 570 \text{ \AA}$ ,  $l_{0a} \geq 4400 \text{ \AA}$ ), and their normals have a Gaussian distribution with a width  $\Delta = 0.664/g_3 = 45' \pm 2'$  at half-maximum, with a center of gravity that coincides with the normal to the sample surface within  $\pm 3'$ , and with a fraction of turbostratification-disordered planes  $p_1 \leq 5.9 \cdot 10^{-3}$ .

b) *Inelastic scattering.* The inelastic scattering intensity of the resonant  $\gamma$  quanta in pyrolytic graphite was measured simultaneously with the elastic scattering by the procedure described above. Measurements were made along the profile of the (002) Bragg reflection and at the maxima of the reflections (004), (006), and (008). The experimental results normalized to the intensity  $I_{00}$  are given in Table II. The intensity of the inelastic scattering at the Bragg peak (002) could not be registered in the interval  $\pm 2^\circ$ .

The experimentally determined ratio  $R_{\text{inel}}$  of the intensity of the inelastic scattering to the intensity of the primary beam can be represented as a sum of the contributions of the thermal diffuse scattering  $R_T$  and of the Compton scattering  $R_C$ . We estimate the latter scattering channel in the free-electron-gas approximation. If we neglect the instrumental errors and the dependence of  $\mu$  on the energy of the scattered quanta, then

$$R_C = \frac{1}{\mu_e} n \sigma_C \Delta \Omega, \quad (5)$$

$$\mu_e(\varepsilon) = \mu + (\mu[\mu + \sigma(1 + \cos^2 2\theta_0)])^{1/2},$$

where  $n$  is the density of the free electrons (four electrons per atom) participating in the Compton scattering,  $\sigma_C$  is the differential cross section of the Compton scattering, and  $\mu_e$  is the effective absorption coefficient and takes into account the attenuation of the primary beam by the secondary extinction. Far from the Bragg direction we have  $\sigma = 0$  and  $\mu_e = 2\mu$ . On the other hand, if the Bragg condition holds, we have, say for (002) reflection of  $^{57}\text{Co}$  radiation, the ratio  $\mu_e(0)/2\mu = 1.6$ , so that the dependence of  $\mu_e$  on  $\varepsilon$  can lead at a small divergence of the primary beam to a dip in the inelastic-scattering intensity at the Bragg peak. With increasing order of the reflection, the corrections needed in (5) to account for  $\sigma$  are small.<sup>1)</sup>

The cross section  $\sigma_C$  was calculated, with only the Fermi screening taken into account, by the procedure of Ref. 9, which yielded the upper bound of  $\sigma_C$ . Under the condition of our experiment, the scattering angles  $\vartheta$  were not large enough to excite the Compton effect on  $K$  electrons, but for all  $\vartheta$  we had  $S = (4\pi/\lambda)\sin\vartheta > k_{\text{cr}}$ , where  $k_{\text{cr}} = 1.4 \text{ \AA}^{-1}$  is the critical wave vector of plasmon excitation,<sup>9</sup> so that the plasmons do not contribute to the inelastic-scattering intensity.

When account is taken of the primary beam-divergence,  $\mu_e$  in (5) must be replaced by  $\mu'_e$ , where  $1/\mu'_e$

is the convolution of  $1/\mu_e(\varepsilon)$  with the instrumental function. Since the horizontal and vertical beam divergences  $\Delta\vartheta$  ( $0.78^\circ$ ) and  $\Delta\varphi$  ( $1.95^\circ$ ) exceed the width  $\varepsilon_0$  of the function  $\sigma(\varepsilon)$ , it can be shown that

$$\frac{2\mu}{\mu'_e} = 2\kappa \left[ 1 + \left\{ 1 + \frac{\sigma(0)}{\mu} (1 + \cos^2 2\theta_0) \right\}^{1/2} \right]^{-1} + (1 - \kappa), \quad (6)$$

where  $\kappa = (\varepsilon_0/2)(\Delta\vartheta^{-1} + \Delta\varphi^{-1})$ ,  $\varepsilon_0 = 0.664/g$ . If, for example, the secondary extinction is negligibly small or  $\varepsilon_0 \ll \Delta\vartheta$  and  $\varepsilon_0 \ll \Delta\varphi$ , then (6) leads to the natural result  $\mu'_e = 2\mu$ . The value of  $R_C$  given in Table II was calculated with account taken of the instrumental errors and of the dependence of  $\mu$  on the energy of the scattered quanta.

The Debye-Waller factor  $\exp(-2M)$ , which was used in the calculation of the elastic and inelastic scattering intensities, was determined by us by using the PG phonon spectrum obtained in Ref. 10 within the framework of the Born-Karman theory. The value of  $M$  obtained for the reflections  $\{00l\}$  in PG at  $T = 293 \text{ K}$  is  $0.383 \sin^2\vartheta/\lambda^2$ .

The value of  $R_T^{(1)}$  of single-phonon scattering by acoustic vibrations with allowance for the anisotropy of the elastic constants was calculated by following mainly Ref. 11. The reciprocal-space volume that contributes to the scattering<sup>11</sup> was approximated by an equivalent sphere of radius  $\tau$ . When estimating the contribution of the optical vibrations to the TDS intensity it must be noted that the dispersion of the optical branches whose polarization is parallel to the scattering vector is negligible inside the sphere of radius  $\tau$ . In this case the ratio of the intensity of TDS by the optical vibration to the intensity of TDS by the acoustic ones is  $k_1 = \omega_L^2/\omega_T^2$ , where  $\omega_L$  and  $\omega_T$  are respectively the frequencies corresponding to  $LA$  phonons with wave-vector modulus  $\tau/2$  and to  $TO_\perp$  phonons in the center of the Brillouin zone, respectively.<sup>12</sup> According to Ref. 13, in the Einstein approximation, the ratio of the second- and first-order TDS intensities is equal to  $M$ . Thus,  $R_T = R_T^{(1)}k$ , where  $k = (1 + k_1)(1 + M)$ .

To reconcile the theory with experiment, we chose the varied parameter to be the shear modulus  $c_{44}$ , whose value, as shown by many measurements of the elastic constants and of the specific heat at low temperatures,<sup>14</sup> depends strongly on the quality of the graphite. The other elastic constants remain practically unchanged on going from natural single-crystal graphite to PG with turbostratified disorder and their values in units of  $10^{11} \text{ dyn/cm}^2$  are<sup>15</sup>  $c_{11} = 106 \pm 2$ ,  $c_{12} = 18 \pm 2$ ,  $c_{13} = 1.5 \pm 0.5$ ,  $c_{66} = 44 \pm 2$ ,  $c_{33} = 3.65 \pm 0.10$ .

Our experimental results have shown that  $c_{44} = (2.5 \pm 0.3) \cdot 10^8 \text{ dyn/cm}^2$ , in agreement with the results obtained for PG in Refs. 14 and 15. The corresponding calculated values of  $R_T^{(1)}$ ,  $R_{\text{inel}}$ , and  $k$  are listed in Table II. For other values of  $c_{44}$ , including all the sets of the elastic constants obtained in Ref. 16, the calculated  $R_{\text{inel}}$  do not agree with experiment.

In conclusion, we summarize the conclusions of Sec. 2b. The existing theory of inelastic scattering with account taken of the anisotropy of the elastic constants

permits a satisfactory description of the experimental results, the elastic constants calculated by using the model of the dynamics of the graphite model in the Born-Karman approximation agrees with experiment within the limits of errors, whereas the elastic constants obtained by the analytic-potential method<sup>16</sup> do not agree with the experimental results. The use of the proposed procedure of inelastic scattering of Mössbauer  $\gamma$  radiation for the study of the properties of PG has shown that this method is effective<sup>2)</sup> when it comes to determining the shear modulus  $c_{44}$  and by the same token the quality of the graphite. This method can be used equally well for the separation of the elastic and inelastic components in scattering with high resolution ( $\sim 10^{-8}$  eV), both in solids and in liquids or gases that do not contain Mössbauer isotopes.

<sup>1)</sup>For 14.4-keV radiation, the ratios  $\sigma(0)/\mu$  for the reflections (002), (004), (006), and (008) are respectively 1.99, 0.32, 0.1, and 0.06.

<sup>2)</sup>The method of scattering thermal neutrons is not effective for the measurement of elastic moduli  $\leq 10^8$  dyn/cm<sup>2</sup>, in view of the small energy resolution,  $\sim 10^{-4}$  eV.<sup>12</sup>

<sup>1)</sup>D. A. O'Connor and N. M. Butt, Phys. Lett. 7, 233 (1963).

<sup>2)</sup>D. C. Champeney and F. W. D. Woodhans, J. Phys. B 1, 260

(1968).

<sup>3)</sup>E. E. Gaubman, Yu. F. Krupyanskiĭ, V. I. Gol'danskiĭ, T. V. Zhuravleva, and I. P. Suzdalev, Zh. Eksp. Teor. Fiz. 72, 2172 (1977) [Sov. Phys. JETP 45, 1141 (1977)].

<sup>4)</sup>N. N. Lobanov, Deposited manuscript, VINITI No. 433-78, Feb. 7, 1978.

<sup>5)</sup>W. H. Zachariasen, Acta Crystallogr. 23, 558 (1967).

<sup>6)</sup>International Tables of X-ray Crystallogr., Kynoch Press, England, 1965.

<sup>7)</sup>L. D. Calvert, R. C. Killean, and A. Mathienson, Acta Crystallogr. Sect. A 31, 855 (1975).

<sup>8)</sup>G. E. Bacon, Acta Cryst. 4, 558 (1951).

<sup>9)</sup>Y. Ohmura and H. Matsudaira, J. Phys. Soc. Jpn. 19, 1335 (1964).

<sup>10)</sup>J. A. Young and J. U. Koppel, J. Chem. Phys. 42, 357 (1965).

<sup>11)</sup>M. Sakata and J. Haradao, Acta Crystallogr. Sect. A 32, 426 (1976).

<sup>12)</sup>R. Nickow, N. Wakabayachi, and H. G. Smith, Phys. Rev. B 5, 4951 (1972).

<sup>13)</sup>W. Cochran, in: Phonons in Perfect Lattices and in Lattices with Point Imperfections, ed. R. W. H. Stevenson, Edinburgh, 1966.

<sup>14)</sup>D. E. Soule and C. W. Nezbeda, J. Appl. Phys. 39, 5122 (1968); B. J. C. Van der Hoeven and P. H. Keesom, Phys. Rev. 130, 1318 (1963).

<sup>15)</sup>O. L. Blakslee, D. G. Proctor, E. J. Seldin, G. B. Spence, and T. Weng, J. Appl. Phys. 41, 3373 (1970).

<sup>16)</sup>H. A. Rafizadeh, S. Yip, and H. Prask, J. Chem. Phys. 56, 5377 (1972).

Translated by J. G. Adashko

## Thermodynamics of electrons in a quantized semimetal film in strong magnetic fields

I. V. Lerner and Yu. E. Lozovik

*Institute of Spectroscopy, Academy of Sciences of the USSR*

(Submitted 26 September 1978)

Zh. Eksp. Teor. Fiz. 76, 1136-1150 (March 1979)

A quantized semimetal film in strong transverse magnetic fields  $H$  is considered. The thermodynamic characteristics of the system are calculated with allowance for the Coulomb interaction. Transitions to the excitonic phase are predicted for certain relationships between  $H$  and the band overlap  $E_g$ , and the phase diagram of the system is calculated. Field-induced rearrangements in equilibrium quasi-two-dimensional semiconductors are also studied.

PACS numbers: 73.60.Fw

Quasi-two-dimensional electron systems in strong transverse magnetic fields  $H$  are now an object of intensive theoretical and experimental study. The interest in them is stimulated by the complete discreteness of the electron spectrum, which gives rise to their highly unusual properties. The phase transitions in such systems have been studied in a number of papers: the magnetic-field-induced crystallization of electrons in inversion layers (see, e.g., Refs. 1-5), the formation of droplets of a nonequilibrium electron-hole ( $e-h$ ) liquid in quasi-two-dimensional semiconductors in strong fields,<sup>6</sup> and the transition of an  $e-h$  plasma to an excitonic phase in such semiconductors<sup>7</sup> and in systems with

separated  $e$  and  $h$  in strong fields.<sup>8</sup>

A special place amongst these "quasi-zero-dimensional" systems is occupied by size-quantized semimetal films<sup>9</sup> in strong fields  $H$ : the properties of such systems have been studied experimentally in a whole series of papers (e.g., Refs. 10 and 11). For a systematic description of the kinetic properties of these systems it is necessary first of all to study the ground state and thermodynamics of the electron Fermi liquid in the films. It is precisely these problems that are considered in the present paper.

We shall confine ourselves to a two-band model of the